Talanta 101 (2012) 396–404

Contents lists available at SciVerse ScienceDirect

Talanta

journal homepage: www.elsevier.com/locate/talanta

Synthesis of highly dispersed mesostructured cellular foam silica sphere and its application in high-performance liquid chromatography

Sha Chen [a], Xiaoqiong Zhang [a], Qiang Han [a,b], Ming Yu Ding [a,*]

[a] Beijing Key Laboratory for Microanalytical Methods and Instrumentation, Department of Chemistry, Tsinghua University, Beijing 100084, China
[b] Laboratory of Fiber Materials and Modern Textile, the Growing Base for State Key Laboratory, Qingdao University, Shandong 266071, China

ARTICLE INFO

Article history:
Received 5 June 2012
Received in revised form
12 September 2012
Accepted 22 September 2012
Available online 28 September 2012

Keywords:
Mesostructured silica
MCF
Morphology
HPLC
Stationary phase

ABSTRACT

Highly dispersed mesostructured cellular foam silica spheres of relatively uniform micrometer size (3.5–4.5 μm) were successfully prepared using a triblock copolymer $EO_{20}PO_{70}EO_{20}$ as the structure-directing agent accompanied by TMB and K_2SO_4. Both two additives have effective influence and K_2SO_4 have better performance than other inorganic salts such as KCl and NaCl. The pore size and surface area were tuned by TMB and NH_4F. The resultant S-MCFs were modified with C_{18} group before being used as the HPLC stationary phase for effective separation of aromatic compounds and phthalic acid esters. The perfect spherical morphology and large pore volume gave rise to low and stable back pressure. High surface area, ultralarge pore size and unique pore structure would permit high flow rates and afford the possibility for fast separation.

1. Introduction

Commercial HPLC columns are usually packed with spherical silica particles. The packing materials exhibit low surface areas ($<500\ m^2/g$) and large pore size distribution which are provided mainly by the inter-particle porosity [1]. Moreover, surface areas continue to decrease when the pore size is further enlarged.

Recently, mesostructured cellular foam (MCF) silica material has attracted a great deal of attention owing to its interconnected pore structure, large pore size, large pore volume ($>1.5\ cm^3/g$) and high surface areas (500–1000 m^2/g) [2,3]. These properties are of great interests for various applications such as adsorption [4–6], separation [7], catalysis [8] and enzyme immobilization [9,10].

In the field of chromatography separation, mesoporous silica has a promising application as a chromatographic stationary phase, in which the crucial parameters are morphology, uniform particle-size, high surface area and well-defined pore size. The high surface area of MCF material can give rise to a high retention of some selected analytes to enhance the HPLC separation efficiency of multi-components. Meanwhile, much larger pore size can also favor the elution of the mobile phase and be potential for separating large biomoleculars while other mesoporous silica materials such as SBA-15, MCM-41 and MSU-1 prepared to be used as HPLC packing materials have pore size <8 nm [11–20]. In addition, comparing to SBA-15 and MCM-41, MCF consists of a three-dimension, interconnected pore structure with ultralarge cells (22–42 nm) and narrower windows (9–22 nm) [2], so intraparticle transport can be facilitated through a 3-dimensional mesoporous structure which may be in favor of fast separation.

In addition to the textural properties, the morphology of the HPLC packing materials also plays an important role. The uniform sphere and 3–5 μm particle-size are basal requirements for the common HPLC packing materials. As a result, many efforts have been devoted in order to improve the morphology of packing materials. According to the previous reports, morphology can be tuned by altering the reaction parameters such as pH, surfactant concentration, the mixture of co-solvent, co-surfactant and electrolyte [21–27]. Mesa et al. modified the synthesis of SBA-15 by using the cetyltrimethyammonium bromide (CTAB) as co-template and ethanol as the co-solvent to prepare micrometer-sized mesoporous spheres [17]. MCM-41 spheres have also been prepared successfully by pseudomorphic synthesis or using co-solvents such as methanol, ethanol and acetone [25–28]. Spherical MSU-1 was prepared through a double-step synthesis by using sodium fluoride and mild acidity [13]. However in previous studies [1], the MCF particles prepared by the conventional method have shown irregular morphology and over 10 μm of particle-size, which are not suitable for chromatographic stationary phases. But for the synthesis of MCF material, only a few reports have focused on the morphology control. Han and co-workers modified the method by cutting the original HCl

* Corresponding author. Tel.: +86 10 62797087; fax: +86 10 62781106.
E-mail address: dingmy@mail.tsinghua.edu.cn (M.Y. Ding).

0039-9140/$ - see front matter © 2012 Elsevier B.V. All rights reserved.
http://dx.doi.org/10.1016/j.talanta.2012.09.047

concentration by half to get the spherical particles [14]. So it is truly necessary to do a real effort on the morphology control of the MCF materials. Additionally, it is still a challenge to prepare highly dispersed spheres due to the fact that using the P123 as the surfactant is easy to obtain the aggregated morphology [13,16,29].

In this paper, a modified method to prepare highly dispersed MCF silica spheres was reported by using K_2SO_4 as the strong electrolytes. The MCF silica spheres prepared have particle-size of 3–5 μm and narrow particle-size distribution. The mutual effects of the electrolytes and the swelling agent (TMB) were both investigated. Before packing into the chromatographic column, the MCF silica spheres were grafted with C_{18} chains by means of the polymerization method to increase the surface hydrophobicity, and the residual hydroxyl was end-capped by hexamethyldisilazane (HMDS). A short HPLC column packed with the C_{18} modified MCF spheres was used for the effective separation of aromatic compounds and phthalic acid esters. The effect of pore size of the MCF on the separation efficiency was also investigated.

2. Experiment

2.1. Chemicals

Pluronic P123 (EO20PO70EO20, M_{av}=5800), tetraethyl orthosilicate (TEOS, 99%) were purchased from Sigma-Aldrich. Octadecyldimethylchlorosilane was obtained from Alfa Aesar. TMB, hydrochloric acid (36.5%), potassium chloride, sodium chloride, potassium sulfate, toluene, acetonitrile, methanol and ethanol were purchased from Beijing Chemical. All chemicals were used directly without further purification.

2.2. Synthesis of mesoporous cellular foam silica spheres

Mesoporous cellular foam (MCF) spheres were synthesized using the triblock copolymer Pluronic P123 as the structure directing agents. In a typical preparation procedure, P123 (2 g) and a certain amount of inorganic salt dissolved in H_2O (60 ml) and concentrated HCl (10 ml) were stirred for more than 2 h to get a transparent solution. Then TMB (1.5, 2.0, 2.5 g) was added under stirring. After 1 h of stirring, TEOS (4.3 g) was added dropwise (12 d/min) and the solution was stirred for another 10 min. The result solution was then transferred to an autoclave and aged at 308 K for 24 h under a static condition, and then kept at 373 K for another 24 h. The precipitate was filtered and washed for three times with deionized water, dried at 333 K and finally calcined at 823 K for 6 h. For the synthesis of S-MCF (1.5[a]), NH_4F (23 mg) in 2 ml water was used as the mineral agent which was added after aging at 308 K for 24 h. All the samples were designated according to Table 1.

Table 1
Synthesis of mesoporous cellular foam silicas and their sample names.

Sample name	Salt species	TMB (g)
MCF-1	KCl	1.5
MCF-2	NaCl	1.5
MCF-3	–	1.5
MCF-4	K_2SO_4	0
S-MCF (1.5)	K_2SO_4	1.5
S-MCF (2.0)	K_2SO_4	2.0
S-MCF (2.5)	K_2SO_4	2.5
S-MCF (1.5[a])	K_2SO_4	1.5

[a] Adding the mineral agent NH_4F.

2.3. Surface modification of the mesoporous cellular foam silica spheres

Octadecyldimethylchlorosilane was used as the surface modification reagent according to a previously reported method [30,31]. The calcined MCF (2.0 g) was pre-evacuated in vacuum at 393 K for 5 h. Then the MCF was dispersed in toluene (200 ml) under N_2. Subsequently, excess octadecyldimethylchlorosilane (6.0 g) was added and the temperature was raised to 383 K after 5 h. This mixture was refluxed for 12 h under N_2. Then HMDS (3 ml) was added and refluxed for another 24 h. The resulting solids were filtered (G4 filter) and washed orderly by toluene and methanol, ethanol for three times. The functionalized MCF silica was dried in the vacuum at 333 K for 7 h.

2.4. Materials characterization

Scanning electron microscopy (SEM) measurement was performed on a FEI Quanta200. Prior to analysis, the sample was placed on a sample holder with an adhesive carbon file and was sprayed with gold (thickness about 15 nm). Nitrogen adsorption–desorption isotherms was performed at 77 K using Micromeritics ASAP 2010 (GA, USA). All the samples before modification were degassed at 473 K for 2 h and C_{18} modified samples were degassed at 393 K for 2 h. The specific surface area was evaluated from nitrogen adsorption data over the relative pressure range from 0.06 to 0.2 using the Brunauer–Emmett–Teller (BET) method. The pore size distribution was calculated using the BJH method although it was known that this method will underestimate the pore diameter. The total pore volume was calculated at relative pressure of 0.99 and the textural properties were listed in Table 2. The BJH pore diameter is defined as the maximum on the pore size distribution curve. Transmission electron microscopy (TEM) measurement was performed using Tecnai $G^2$20 (FEI, USA) with an acceleration voltage of 200 kV and a point resolution of 0.24 nm. Prior to the TEM imaging, the MCF spheres were grind into fragments, well dispersed in ethanol under ultrasonic and then dried on carbon-coated Cu grid.

The carbon and hydrogen contents of the functionalized MCF samples were determined by a CE-440 Elemental Analyzer (USA) and the infrared (IR) spectrum was measured with a Perkin Elmer spectrum GX FT-IR system. Thermogravimetric analysis (TGA, Netzsch TG 209 F3 Tarsus) for the samples was carried out in the range of 35 °C–900 °C at the rate of 10 °C per minute with air as the purge gas.

2.5. Chromatography application of C_{18} modified MCF silica spheres

The obtained C_{18} modified MCF silica spheres were slurry-packed into a stainless-steel tubes ($100 \times 4.6\ mm^2$ ID) using

Table 2
Nitrogen adsorption–desorption parameters for MCF silica.

Sample	Pore size (nm)[a]	Window size (nm)[a]	Surface area (m^2/g)	Pore volume (cm^3/g)
MCF-1 (KCl)	29.7	8.8	499	1.57
MCF-2 (NaCl)	29.1	8.8	440	1.38
MCF-3(without salt)	37.6	7.0	659	1.16
S-MCF (1.5)	22.7	9.0	716	1.64
S-MCF (2.0)	23.2	8.6	621	1.51
S-MCF (2.5)	28.6	9.0	655	1.68
S-MCF (1.5[b])	30.0	13.0	442	1.76

[a] The pore size and the window size were derived from the adsorption and desorption branch separately using the BJH method separately.
[b] Adding the mineral agent NH_4F.

chloroform as homogenate solvent at 40 MPa. Ethanol was used to push the slurry into the column.

All chromatography experiments were performed on the Agilent 1100 HPLC equipped with a quaternary pump, Rheodyne 7725i injector with 20 μl sample loop and variable wavelength detector (VWD). Five aromatic compounds (naphthalene, fluoranthene, benzo[a]anthracene, benzo[b]fluoranthene and benzo[a]pyrene) were separated on the column using acetonitrile/water (70/30, v/v) as the mobile phase at the flow rates of 0.8–3.0 ml/min with the UV detection at 254 nm. Three phthalic acid esters (PAEs) DMP, DEP, DBP were separated on the column using acetonitrile/water (70/30, v/v) as the mobile phase at the flow rate of 1.0 ml/min with the UV detection at 226 nm.

3. Results and discussion

3.1. Synthesis and characterization of the MCF silica spheres

Morphological control of the MCF is the main subject in this research due to the fact that the overall morphology is as important as the internal structure. The morphology of the MCF particles prepared by the conventional method was irregular and the size was usually over 10 μm, which is not available for the common HPLC packing materials [2]. To synthesize the spherical MCF, Han modified the method by cutting the original HCl concentration by half [32]. We have successfully prepared highly dispersed MCF spheres with the particle-size of 3–5 μm and narrow particle-size distribution by using the K_2SO_4 as the strong electrolyte (Fig. 1A). To examine how salts effect on the synthesis process, the MCF silica particles were synthesized using K_2SO_4, KCl, NaCl as salt species and in the absence of any salt, respectively while other reaction conditions were kept the same. As a result, relatively large difference on the morphology is examined (Fig. 1). Using KCl (Fig. 1B) and NaCl (Fig. 1C) as the salt species gave rise to the similar spherical morphology with relatively serious aggregation while the addition of K_2SO_4 formed the highly dispersed spheres (Fig. 1A). Notably, MCF materials prepared with the conventional method without adding any salt in this article have the irregular agglomerate particles (>10 μm) consist of small particles of 0.5–1 μm (Fig. 1D) which were identical to the previous report [2].

In our research, it was observed that the mixing solution without any salt turned into white emulsion immediately right after adding TMB while the other reactions with any kind of salt need about 10 min to have the same phenomena. Above results can illustrate that salts such as KCl, NaCl, K_2SO_4 can increase the time of the formation of the O/W emulsion because to our known knowledge, the MCF synthesis is more likely a nonaqueous emulsion templating route [2,33,34]. Consequently, experimental conditions increasing the induction time may increase the curvature of the resulting morphology such as forming spheres [23].

In order to investigate the role TMB played in the prepared process, variable amounts of the TMB of 0, 1.5, 2.0, 2.5 g were used when the amount of K_2SO_4 was kept the same. The results were shown in Fig. 2. An obvious difference in morphology can be observed when comparing the SEM image of Fig. 2A and Fig. 2B which were corresponding to the samples whether adding TMB or not. Sample prepared without adding TMB was nubby together with the low yield of microspheres (Fig. 2A). Both of S-MCF (1.5) (Fig. 2B) and S-MCF (2.0) (Fig. 2C) have perfect microspheres together with high yield of almost 100%. While increasing the

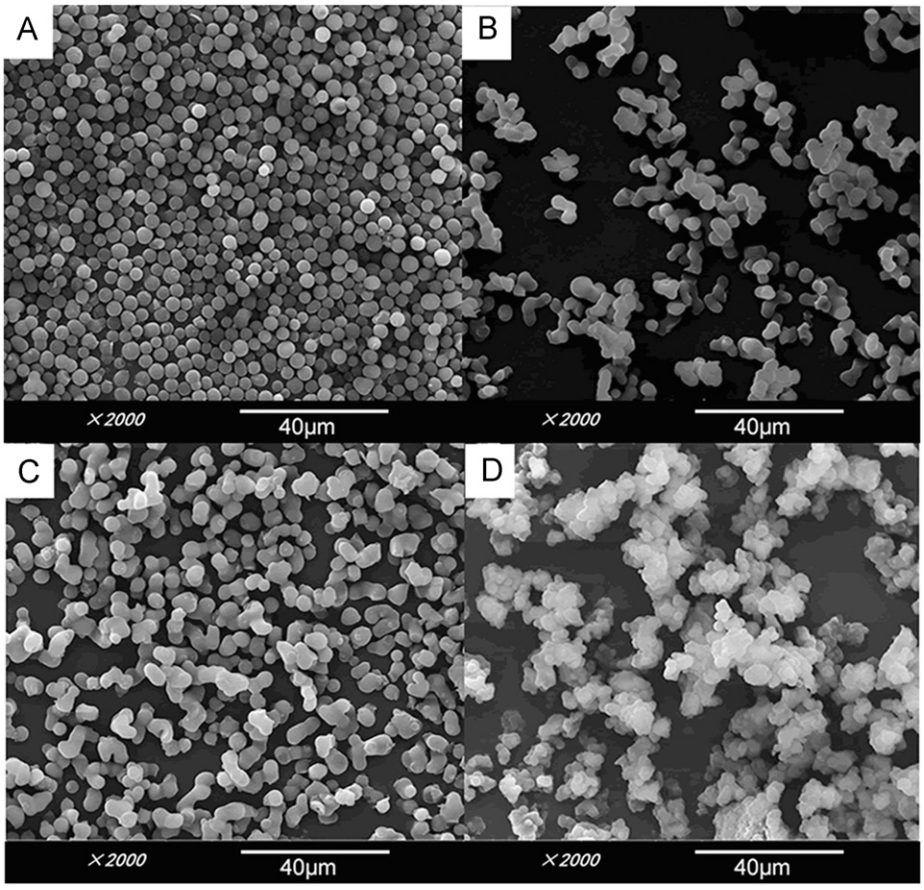

Fig. 1. SEM images of MCF silica using different salt species (A) S-MCF (1.5); (B) MCF-1; (C) MCF-2; (D) MCF-3.

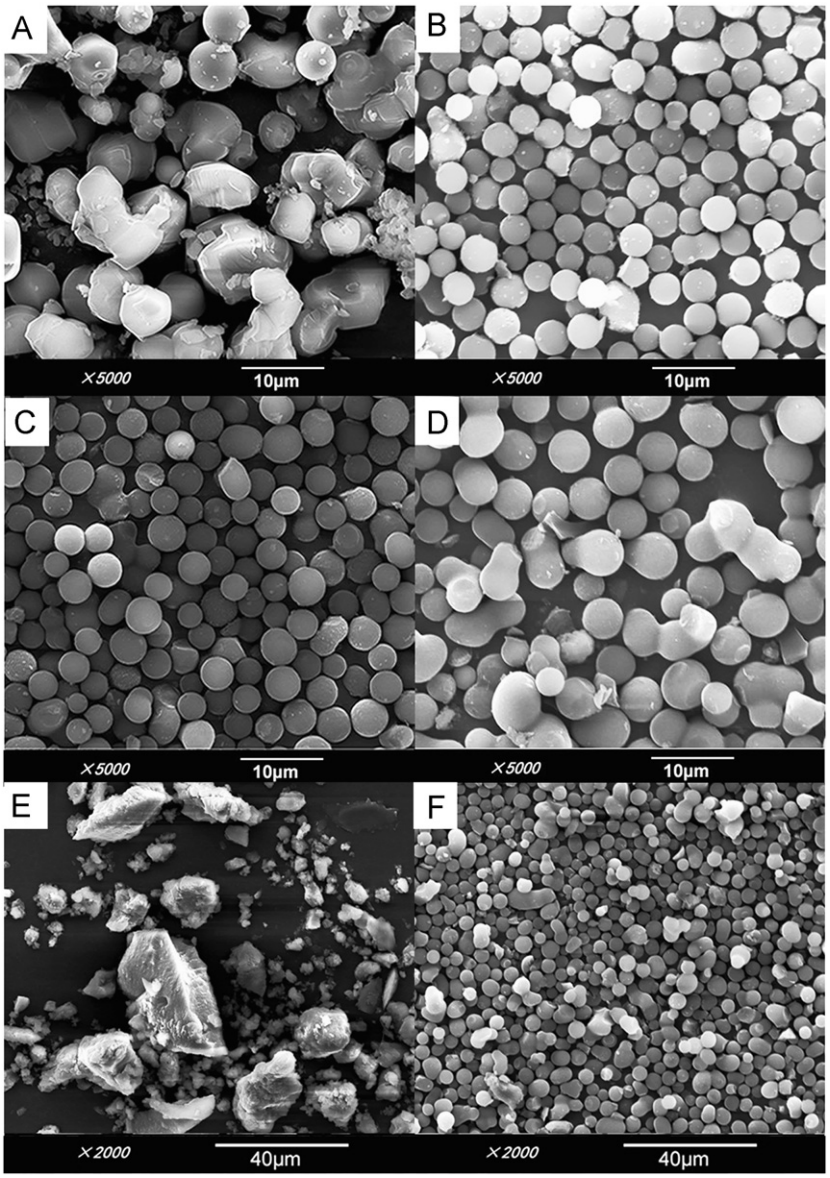

Fig. 2. SEM images of MCF silica using different amounts of TMB (A) MCF-4; (B) S-MCF (1.5); (C) S-MCF (2.0); (D) S-MCF (2.5); (E) adding NH_4F in the self-assembly; (F) adding NH_4F after aging at 308 K.

amount of TMB to 2.5 g, it has a negative effect on the formation of dispersed microspheres (Fig. 2D). Therefore, 1.5 g and 2.0 g TMB were the optimal amounts in this synthesis method. In conclusion, both K_2SO_4 and TMB are necessary for the formation of high yield dispersed microspheres. By contrast, K_2SO_4 was more crucial than TMB in our research which may have an opposite consequence with the previous report in which KCl was used as the salt to obtain spheres. In the previous literature, the conclusion that TMB has a more important influence on the formation of spherical morphology of SBA-15 than KCl was drawn [18].

In this work, NH_4F was used as the mineralizing agent to increase the window size. For the purpose of obtaining spherical silica particles, the adding time of NH_4F is extremely important. NH_4F should be added right after relatively low temperature aging, otherwise irregular agglomerate particles were formed if adding in the self-assembly time (Fig. 2E, F).

Nitrogen adsorption–desorption isotherms of the calcined MCF silica spheres are shown in Fig. 3, and the derived pore size distributions obtained from the adsorption and desorption branch separately using the BJH method are shown in Fig. 4. The textural properties are summarized in Table 2. All the samples exhibit type IV isotherms with clear capillary condensation steps indicating mesoporous structures. The P/P_0 positions of the inflection points are related to the diameter of mesoporous particles. The sharpness of the step indicates the uniformity of the mesoporous structure. For the samples prepared with salts all have relatively more uniform size distribution than MCF-3 prepared without any salt which can be recognized from the adsorption–desorption isotherms (Fig. 3) and the pore size distribution (Fig. 4). The difference can be contributed to the Hofmister effect which illustrates that anions like Cl^-, SO_4^{2-} can help to form more stable micelles in aqueous solution. However, cell size was decreased after the addition of any kind of salt. When altering the amounts of the TMB, cell size was increased while window size almost stayed the same in accordance with the previous literatures [2,3]. In this study, NH_4F was used to enlarge the window size. As can be seen from Table 2, an increased cell size of 30.0 nm and window size of 13 nm were obtained in comparison with sample S-MCF (1.5) of 22.7 nm cell size and 9.0 nm window size when

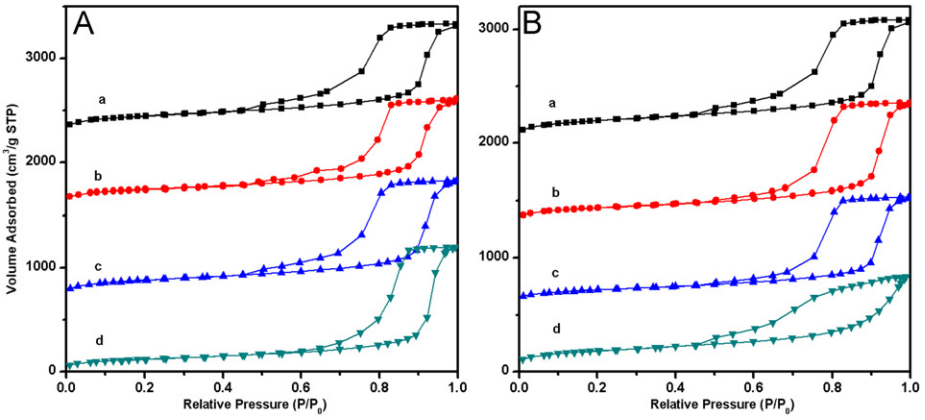

Fig. 3. Nitrogen adsorption and desorption isotherms of calcined MCF (A) using different salt species (a) S-MCF (1.5); (b) MCF-1; (c) MCF-2; (d) MCF-3. (B) using different TMB amounts (a) S-MCF (1.5); (b) S-MCF (2.0); (c) S-MCF (2.5); (d) S-MCF(1.5[a]).

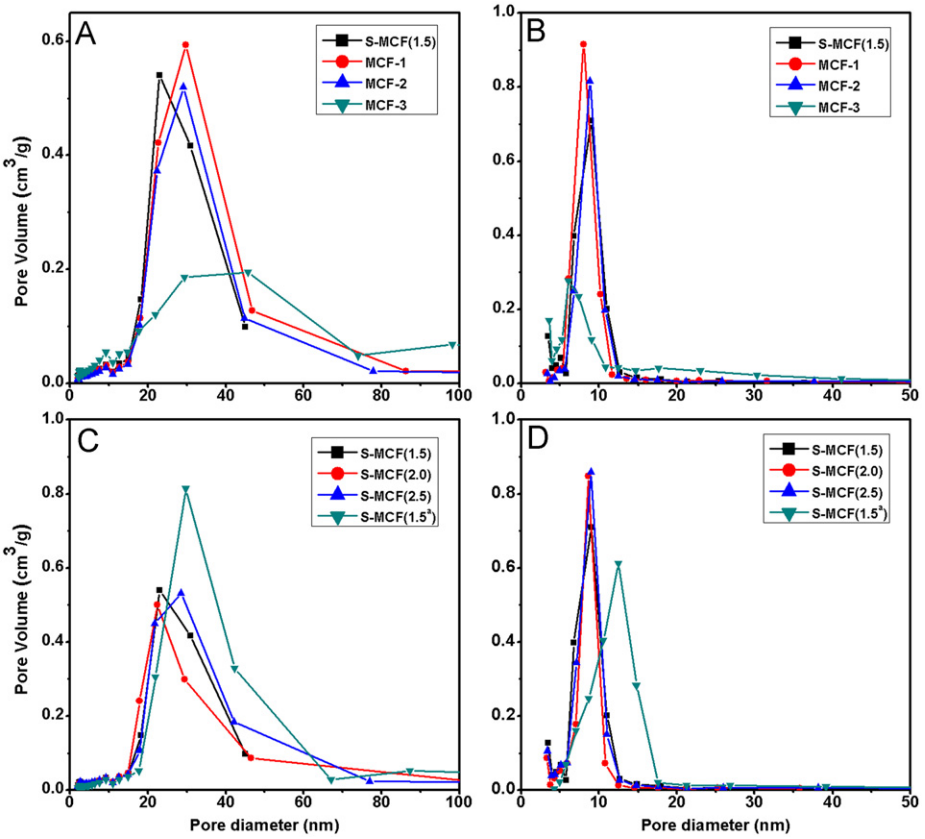

Fig. 4. Pore size distributions of MCF silica (A) cell size of MCF silica with different salt species; (B) window size of MCF silica with different salt species; (C) cell size of MCF silica with variable amounts of TMB; (D) window size of MCF silica with variable amounts of TMB[a] adding the mineral agent NH_4F.

using NH_4F. But the surface area decreased from 716 m^2/g to 442 m^2/g at the same time. It is noted that pore volume for S-MCF (1.5) and S-MCF (1.5[a]) are 1.64, 1.76 cm^3/g, respectively, higher than MCF-3 (1.16 cm^3/g) and reported SBA-15(1.05 cm^3/g) [35,36].

The three-dimensional, interconnected pore structure of MCF was also confirmed by the high-resolution TEM as shown in Fig. 5. The cell size can be estimated to be about 23 nm and the window size was nearly 9.0 nm which was in good agreement with the result calculated from the nitrogen adsorption measurement. The schematic diagram of the synthesis process was illustrated in Fig. 6. The proposed formation mechanism can be suggested as the following three stages. (1) The formation of the oil-in-water microemulsions consisting of TMB/P123 droplets. In this stage, the droplet size can be influenced by the concentration of the TMB and thus control the diameter of the cells. (2) The hydrophobic TEOS hydrolyze around the surface of the TMB/P123 droplets to form hydrophilic Si–OH ($Si–OH_3^+$). Ethanol acts as the co-solvent to reduce the free energy and thus increase the curvature. Meanwhile, the hydrophilic silica begins to condense slowly through hydrogen bond. (3) When increasing the temperature, the hydrophilic silica continues to condense while the silica–TMB/P123 composites come into agglomeration. The windows interconnecting the cells may form in the regions where neighboring composites come into each other. After calcination, the unique three-dimensional mesostructured cellular foam was obtained.

3.2. Surface modification of the MCF silica spheres and its application in HPLC

The IR spectra of MCF after surface modification was shown in Fig. 7. Three strong peaks at 2962, 2929 and 2858 cm^{-1} were corresponding to the stretching of CH_3 and CH_2, and a weak peak at 1460 cm^{-1} is the bending vibration of the C–H. The above results can confirm the existence of the C_{18}. For the sample S-MCF (1.5[a]), the typical peaks at 2961, 2927 and 2856 cm^{-1} can also prove the successfully grafted of C_{18} group.

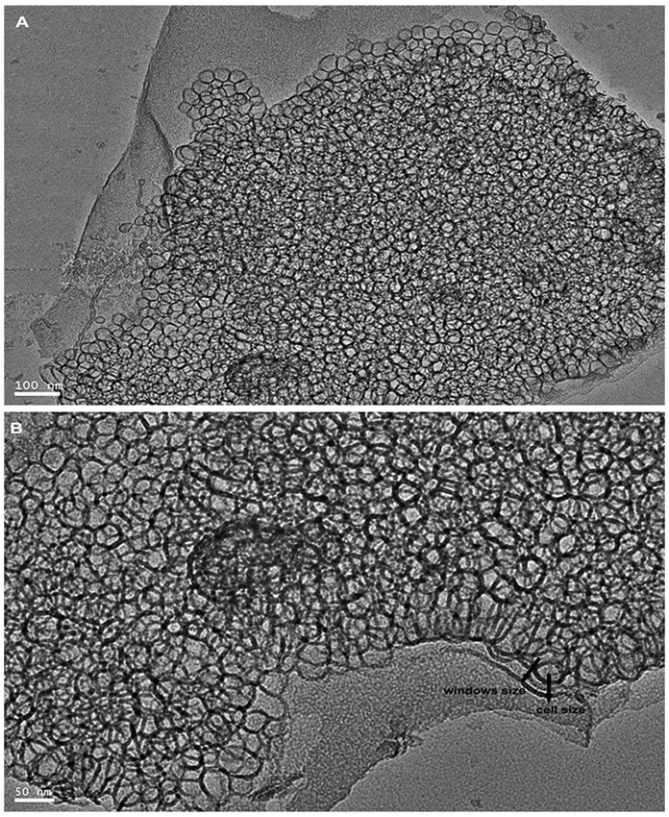

Fig. 5. TEM images of S-MCF (1.5) (A) scale bar: 100 nm; (B) scale bar: 50 nm.

The total contents of carbon and hydrogen of the C_{18}-S-MCF (1.5) and C_{18}-S-MCF (1.5[a]) were determined to be 17.3% and 16.8%, respectively by elemental analysis. Additionally, thermogravimetric analysis was also used to determine the amount of organic functional groups, as shown in Fig. 8. The loss of the weight of all the samples below 100 °C attributes to the loss of adsorbed water. Comparing to the original MCF, the C_{18}-S-MCF (1.5) and C_{18}-S-MCF (1.5[a]) silica materials both have the highest weight loss of 17% on the corresponding TG and DTG curves between 200 °C and 500 °C, which are in accordance with the elemental analysis results.

C_{18}-S-MCF (1.5) and C_{18}-S-MCF (1.5[a]) were used as the stationary phase of reversed-phase HPLC for separation of aromatic compounds and phthalic acid esters. The separation

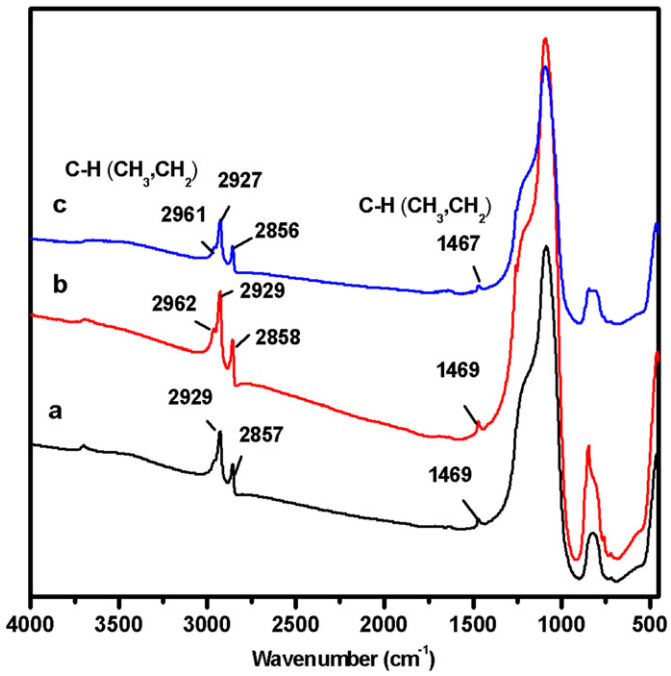

Fig. 7. FTIR spectra of MCF (a) S-MCF (1.5) after modification with C_{18} group; (b) S-MCF (1.5) after endcapping with HMDS; (c) S-MCF (1.5[a]) after modification and endcapping.

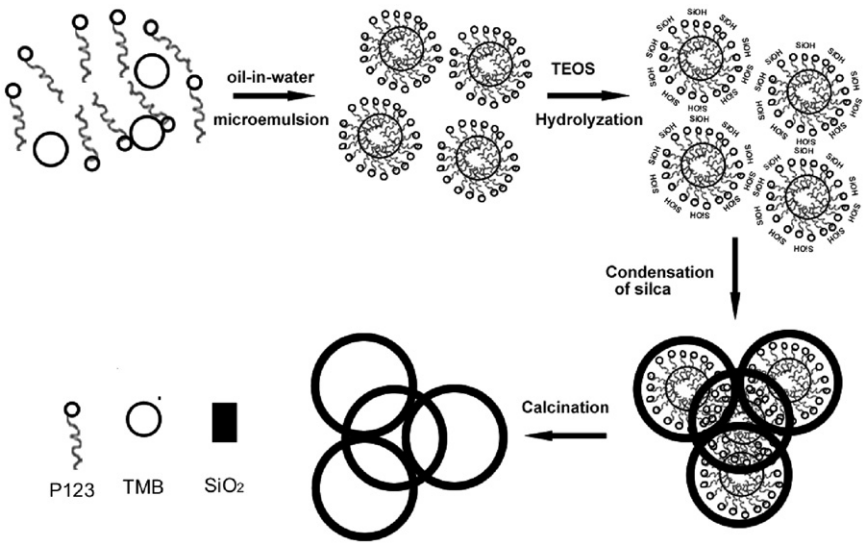

Fig. 6. Schematic diagram of the proposed assembly process and the formation of the mesoporous structure of the MCF material.

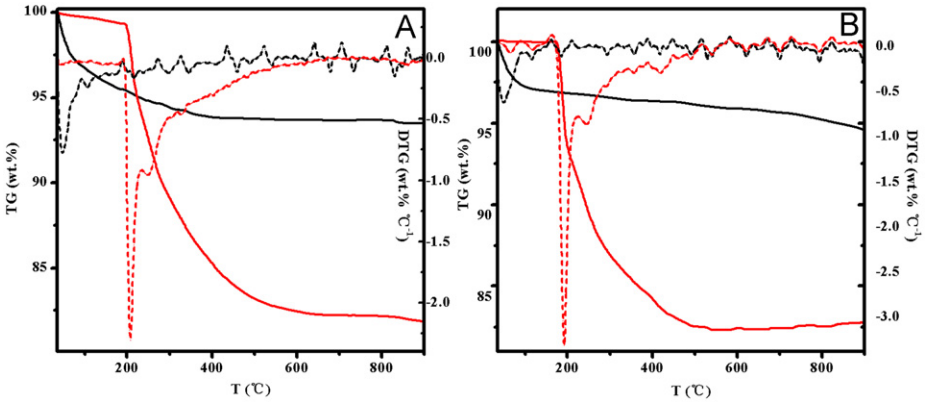

Fig. 8. TG and DTG curves for the original (black lines) and C_{18}-grafted (red lines) of MCF silica (A) S-MCF (1.5); (B) S –MCF (1.5[a]). (For interpretation of the references to color in this figure, the reader is referred to the web version of this article.)

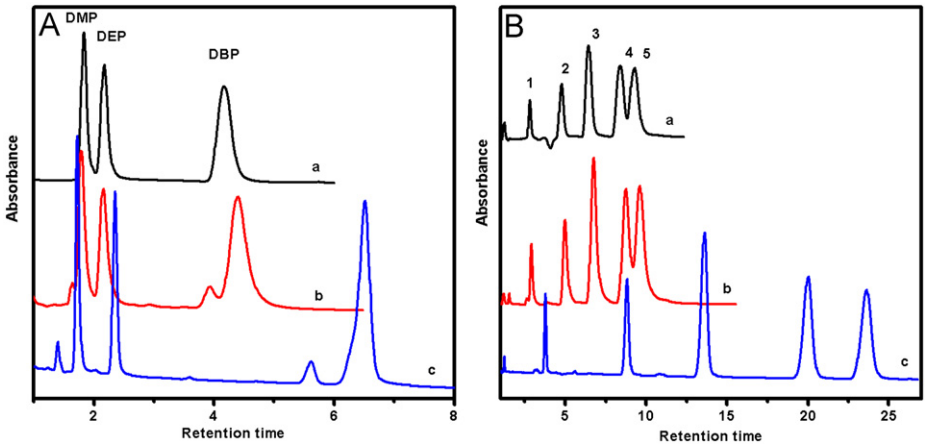

Fig. 9. Separation of (A) three phthalic acid esters (PAE) standards and (B) nonpolar alkyl aromatic compounds. (A) Column conditions: 100 × 4.6 mm^2 i.d. Mobile phase: acetonitrile/H_2O mixture (70/30: v/v); flow rate:1.0 ml/min. UV detection at 226 nm; (B) Peaks from left to right: naphthalene, fluoranthene, benzo[a]anthracene, benzo[b]fluoranthene and benzo[a]pyrene. Column conditions: 100 × 4.6 mm^2 i.d. Mobile phase: acetonitrile/H_2O mixture (70/30. v/v). UV detection at 254 nm. (a) C_{18}-MCF (1.5[a]); (b) C_{18}-S-MCF (1.5); (c) Kromasil C18.

Table 3
Retention capacity of home-made columns and commercial column for several solutes under the same separation conditions.

Solutes	k' (MCF-1.5a)	k' (MCF1.5)	k' (kromasil)	$k'_{(kromasil)}/k'^{a}_{(MCF-1.5}$	$k'_{(kromasil)}/k'_{(MCF1.5)}$
DMP	1.07	1.41	2.05	1.9	1.5
DEP	1.46	1.90	3.16	2.1	1.7
DBP	3.72	4.92	10.51	2.8	2.1
Naphthalene	1.34	1.63	3.41	2.5	2.1
Fluoranthene	2.97	3.51	5.50	1.9	1.6
Benzo[a]anthracene	3.69	5.11	9.28	2.5	1.8
Benzo[b]fluoranthene	5.98	6.91	14.85	2.5	2.1
Benzo[a]pyrene	6.70	7.70	26.51	4.0	3.4

properties of our home-made columns were compared with a commercial HPLC packing material (Kromasil C18), which exhibits good spherical morphology and textual properties (5 μm, 10 nm, 350 m^2/g, 1.0 cm^3/g). As shown in Fig. 9, base-line separations with the same eluting order of solutes were obtained for both the home-made columns and commercial Kromasil C18 column under the same separation conditions. Additionally, almost the same separating performance and comparable elution peak shape are obtained between the two home-made columns

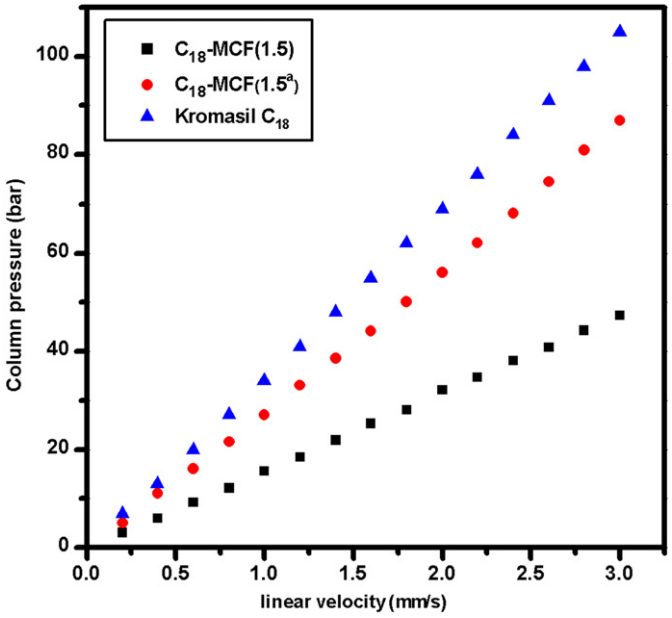

Fig. 10. The pressure for benzo[a]anthracene on columns. Column conditions: 100 × 4.6 mm^2 i.d. Mobile phase: acetonitrile/H_2O mixture (70/30. v/v). UV detection at 254 nm.

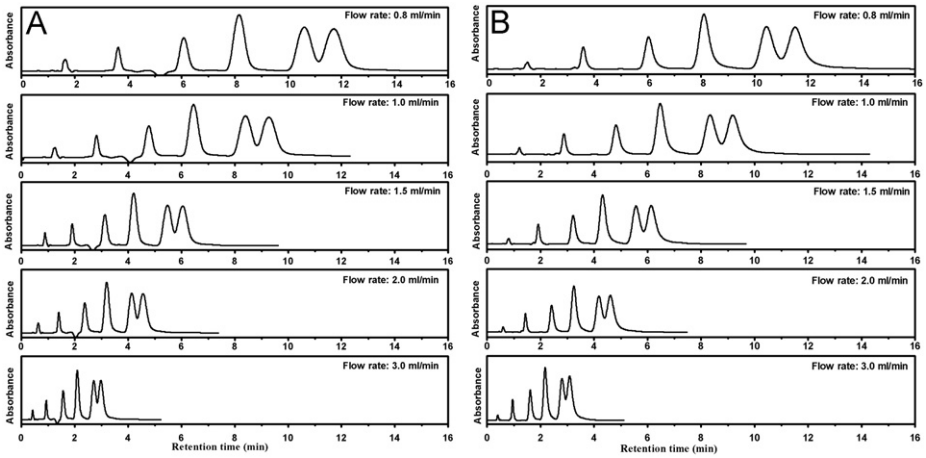

Fig. 11. Separation of nonpolar alkyl aromatics at the flow rates of 0.8 ml/min, 1.0 ml/min, 1.5 ml/min, 2.0 ml/min and 3.0 ml/min. Peaks from left to right: naphthalene, fluoranthene, benzo[a]anthracene, benzo[b]fluoranthene and benzo[a]pyrene. Column conditions: 100 × 4.6 mm^2 i.d. Mobile phase: acetonitrile/H_2O mixture (70/30. v/v). UV detection at 254 nm. (A) C_{18}-MCF (1.5[a]); (B) C_{18}-S-MCF (1.5).

and the commercial HPLC column. It is worth mentioning that C_{18}-S-MCF (1.5) and C_{18}-S-MCF (1.5[a]) silica particles gave more symmetrical peak shape of DBP compared with the commercial silica particles.

The retention factor (k') for each molecule is summarized in Table 3. Compared with the commercial column, the home-made columns have a lower retention factor (k') although the coverage of C_{18} is almost the same. It may be because of the largely decrease of the surface area after surface modification which has also been reported by the previous articles [14,16,18]. Moreover, by considering the surface areas ratios, Kromasil (350 m^2/g) are 2.1 times higher than the C_{18}-S-MCF-1.5[a] (171 m^2/g) and 1.6 times higher than C_{18}-S-MCF-1.5 (214 m^2/g) which are approximately in accordance with the retention factor ratios (k') in Table 3. However, as shown as in Table 3, solute benzo[a]pyrene exhibits a much lower retention factor in contrast to other solutes which may attribute to the much larger pore size (21.6 nm and 28.8 nm) of the prepared MCF packing materials after modification which facilitates mass transport. Therefore, compared to commercial packing silica spheres, the prepared MCF silica spheres with large pore size may be very advantageous in case of strongly retained solutes to shorten analysis time.

As was shown in Fig. 10, our home-made columns have low back pressure and good linearity at different linear velocities which can indicate the excellent spherical morphology. The good stability and low back pressure can also afford the possibility for the fast separation. What's more, the prepared MCF columns exhibit lower pressure with the same packing method comparing with the commercial column, which have good prospect to be used in UPLC. The investigation of separation of the aromatic compounds at a series of flow rates on C_{18}-S-MCF (1.5) and C_{18}-S-MCF (1.5[a]) was shown in Fig. 11. As can be seen, both column C_{18}-S-MCF (1.5) and column C_{18}-S-MCF (1.5[a]) of 4.6 × 100 mm^2 provide effective separation of aromatic compounds even at the flow rate of 3.0 ml/min. The ultralarge pore size and unique pore structure of MCF materials do present advantage on fast separation.

4. Conclusion

Highly dispersed mesostructured cellular foam silica spheres of relatively uniform micrometer size (3.5–4.5 μm) were successfully prepared with the assistance of K_2SO_4 and TMB. K_2SO_4 performed better than NaCl, KCl and the addition of salt can also increase the uniformity of the pore size distribution. Window size can be tuned by NH_4F and the adding time influenced greatly on the morphology. S-MCF spheres were applied in HPLC after modified with C_{18} and both columns C_{18}-S-MCF (1.5) and C_{18}-S-MCF (1.5[a]) exhibit excellent separation for aromatic compounds and phthalic acid esters without any obvious difference in retention time. The ultralarge pore size and unique pore structure of MCF materials do present advantage on fast separation in HPLC and have prospect to be used in UPLC when comparing to the commercial silica particles.

Acknowledgment

This project was supported by the National Nature Science Foundation of China (No 21075074).

References

[1] K.W. Gallis, J.T. Araujo, K.J. Duff, J.G. Moore, C.C. Landry, Adv. Mater. 11 (1999) 1452–1455.
[2] P. Schmidt-Winkel, W.W. Lukens, D.Y. Zhao, P.D. Yang, B.F. Chmelka, G.D. Stucky, J. Am. Chem. Soc. 121 (1999) 254–255.
[3] P. Schmidt-Winkel, W.W. Lukens, P.D. Yang, D.I. Margolese, J.S. Lettow, J.Y. Ying, G.D. Stucky, Chem. Mater. 12 (2000) 686–696.
[4] J.S. Kin, R.J. Desch, S.W. Thiel, V.V. Guliants, N.G. Pinto, Micropor. Mesopor. Mater. 149 (2012) 60–68.
[5] J.S. Kin, R.J. Desch, S.W. Thiel, V.V. Guliants, N.G. Pinto, J. Chromatogr. A. 1218 (2011) 6697–6704.
[6] H.H. Wan, J.Y. Yan, L. Yu, X.L. Zhang, X.Y. Xue, X.L. Li, X.M. Liang, Talanta 82 (2010) 1701–1707.
[7] Y. Han, S.S. Lee, J.Y. Ying, Chem. Mater. 19 (2007) 2292–2298.
[8] D.M. Jiang, J.S. Gao, J. Li, Q.H. Yang, C. Li, Micropor. Mesopor. Mater. 113 (2008) 385–392.
[9] X. Zhang, R.F. Guan, D.Q. Wu, K.Y. Chan, J. Mol. Catal. B: Enzym. 33 (2005) 43–50.
[10] J.Q. Zhao, Y.J. Wang, G.S. Luo, S.L. Zhu, Bioresour. Technol. 101 (2010) 7211–7217.
[11] T. Martin, A. Galarnear, F.D. Renzo, D. Brunel, F. Fajula, Chem. Mater. 16 (2004) 1725–1731.
[12] C. Thoelen, J. Paul, I.F.V. Vankelecom, P.A. Jacob, Tetrahedron: Asymmetry 11 (2000) 4819–4823.
[13] B.C. Boissière, M. Kümmel, M. Persin, A. Larbot, E. Prouzet, Adv. Funct. Mater. 11 (2001) 129–135.
[14] Y. Han, S.S. Lee, J.Y. Ying, J. Chromatogr. A 1217 (2010) 4337–4343.
[15] X.B. Liu, L.S. Li, Y. Du, Z. Guo, T.T. Ong, Y. Chen, S.C. Ng, Y.H. Yang, J. Chromatogr. A 1216 (2009) 7767–7773.
[16] Y.R. Ma, L.M. Qi, J.M. Ma, Y.Q. Wu, Q. Liu, H. Cheng, Colloids Surf. A 229 (2003) 1–8.
[17] M. Mesa, L. Sierra, B. Lopez, A. Ramirez, J.L. Guth, Solid. State. Sci. 5 (2003) 1303–1308.

[18] H.H. Wan, L. Liu, C. Li, X.Y. Xue, X.M. Liang, J. Colloid. Interface Sci. 337 (2009) 420–426.
[19] Y.Y. Li, S.Y. Cheng, P.C. Dai, X.M. Liang, Y.X. Ke, Chem. Comm. (2009) 1085–1087.
[20] Y.X. Zhao, Y.M. Ding, D.P. Chen, Anal. Chim. Acta. 542 (2005) 193–198.
[21] Z.X. Cao, J. Zhang, J.L. Zeng, L.X. Sun, F. Xu, Z. Cao, L. Zhang, D.W. Yang, Talanta 77 (2009) 943–947.
[22] D.Y. Zhao, J.Y. Sun, Q.Z. Li, G.D. Stucky, Chem. Mater. 12 (2000) 275–279.
[23] C.Z. Yu, J. Fan, B. Tian, D.Y. Zhao, Chem. Mater. 16 (2004) 889–898.
[24] M. Grün, K.K. Unger, A. Matsumoto, K. Tsutsumi, Micropor. Mesopor. Mater. 27 (1999) 207–216.
[25] Q. Cai, Z.S. Luo, W.Q. Pang, Y.W. Fan, X.H. Chen, F.Z. Cui, Chem. Mater. 13 (2001) 258–263.
[26] B. Pauwels, G.V. Tendeloo, C. Thoelen, W.V. Rhijn, P.A. Jacobs, Adv. Mater. 13 (2001) 1317–1320.
[27] T. Martin, A. Galarneau, F.D. Renzo, D. Brunel, F. Fajula, Chem. Mater. 16 (2004) 1725–1731.
[28] M. Grün, I. Lauer, P. Klaus, K. Unger, Adv. Mater. 9 (1997) 254–257.
[29] W.J.J. Stevens, K. Lebeau, M. Mertens, G.V. Tendeloo, P. Cool, E.F. Vansant, J. Phys. Chem. B 110 (2006) 9183–9187.
[30] K. Kailasam, K. Müller, J. Chromatogr. A 1191 (2008) 125–135.
[31] R.J. Tian, J.M. Sun, H. Zhang, M.L. Ye, Electrophoresis 27 (2006) 742–748.
[32] Y. Han, S.S. Lee, J.Y. Ying, Chem. Mater. 19 (2007) 2292–2298.
[33] A. Imhof, D.J. Pine, Nature 389 (1997) 948–951.
[34] A. Imhof, D.J. Pine, Adv. Mater. 10 (1998) 697–700.
[35] J.W. Zhao, F. Gao, Y.L. Fu, W. Jin, P.D. Yang, D.Y. Zhao, Chem. Commun. (2002) 752–753.
[36] F. Gao, J.W. Zhao, S. Zhang, F. Zhou, W. Jin, X.M. Zhang, P.Y. Yang, D.Y. Zhao, Chem. J. Chin. Univ. 23 (2002) 1494–1497.